HAL open science

Electric field emitted by a particle track in two semi-infinite media

Daniel García-Fernández, Richard Dallier, Antony Escudie, Lilian Martin, Benoît Revenu

To cite this version:

Daniel García-Fernández, Richard Dallier, Antony Escudie, Lilian Martin, Benoît Revenu. Electric field emitted by a particle track in two semi-infinite media. 36th International Cosmic Ray Conference, Jul 2019, Madison, United States. pp.268, 10.22323/1.358.0268 . hal-02903391v1

HAL Id: hal-02903391

https://hal.science/hal-02903391v1

Submitted on 11 Nov 2020 (v1), last revised 21 Jul 2020 (v2)

HAL is a multi-disciplinary open access archive for the deposit and dissemination of scientific research documents, whether they are published or not. The documents may come from teaching and research institutions in France or abroad, or from public or private research centers.

L'archive ouverte pluridisciplinaire **HAL**, est destinée au dépôt et à la diffusion de documents scientifiques de niveau recherche, publiés ou non, émanant des établissements d'enseignement et de recherche français ou étrangers, des laboratoires publics ou privés.

PROCEEDINGS OF SCIENCE

Electric field emitted by a particle track in two semi-infinite media

Daniel García-Fernández* [a,b], **Richard Dallier** [c,d], **Antony Escudie** [c], **Lilian Martin** [c,d], **Benoît Revenu** [c,d]

a DESY, Platanenallee 6, 15738, Zeuthen, Germany
b ECAP, Friedrich-Alexander-Universität Erlangen-Nürnberg, Erlangen, Germany
c SUBATECH, Institut Mines-Telecom Atlantique, CNRS/IN2P3, Université de Nantes, Nantes, France
d Unité Scientifique de Nançay, Observatoire de Paris, CNRS, PSL, UO/OSUC, Nançay, France

E-mail: daniel.garcia@desy.de

The radio technique for the detection of cosmic rays is nowadays a well-established experimental technique, and several projects intend to adapt it for the detection of neutrinos. When a primary particle interacts with a target particle in a medium, a shower containing electrically charged particles is created, and an electric field is emitted. The measurement and analysis of this electric field can reveal the properties of the primary particle. In order to be able to produce an accurate reconstruction of the properties of the primary particle, a reliable calculation of the electric field is needed. Although almost every current radio detection experiment is located near a boundary (e.g. ground), the effect of this boundary on the calculation of the electric field is either not taken into account or the field is decomposed into direct, reflected and transmitted components, which is a correct description in the far-field approximation only. When the emitting shower and the detector are close to the boundary with respect to the observation wavelength, this approximation breaks down, as it is the case for the EXTASIS experiment when the particles are near ground level. We present in this work a frequency-domain calculation of the electric field from a charged particle track lying in two semi-infinite media separated by a planar boundary. We also give an estimate of the expected signal from a full air shower using a toy model.

36th International Cosmic Ray Conference -ICRC2019-
July 24th - August 1st, 2019
Madison, WI, U.S.A.

*Speaker.

© Copyright owned by the author(s) under the terms of the Creative Commons Attribution-NonCommercial-NoDerivatives 4.0 International License (CC BY-NC-ND 4.0).

PoS(ICRC2019)268

1. Introduction

The radio detection of neutrinos and cosmic rays consists in the detection of these particles by measuring the electric field emitted when they interact in a medium. After the interaction, a particle shower containing charged particles is created, and these particles create an electric field that is detectable in the MHz-GHz frequency range.

The radio technique is well-established nowadays as a method of detecting cosmic rays [1], allowing the reconstruction of arrival direction, energy and composition, the three most relevant characteristics of a cosmic ray [2, 3]. Experiments such as CODALEMA [4], LOFAR [5], AERA [6], or Tunka-Rex [7] continue to exploit this technique in a satisfactory way.

Radio can also help with the detection of ultra-high-energy (UHE) neutrinos. Since this kind of detection requires an increase in the effective volume that is prohibitive for the optical detection method, alternative methods become necessary. The radio technique allows the instrumentation of large effective volumes of ice, given that the attenuation length of radio waves in ice is $\sim 1\,\mathrm{km}$. Pathfinder experiments such as ARIANNA [8], ARA [9], and ANITA [10] have paved the way for projected experiments such as RNO.

The radio technique relies heavily on the use of simulations, which constitute the only way of calculating the field from the billions of particles present in a shower. Monte Carlo codes such as SELFAS3, ZHAireS or CoREAS allow the calculation of the field from extensive air showers, while ZHS and, quite recently, NuRadioMC [11], can be used for knowing the neutrino-induced field in dense media.

ZHAireS and NuRadioMC take into account the reflection of the electromagnetic waves on the interface between two media when it is relevant. However, all of the mentioned codes assume that the electric field can be approximated by the radiation field (or far field) only. This hypothesis is valid as long as the distance between the observer and the radiating charges is large compared to the observation wavelength. While this is the case for most experiments, at EXTASIS [12] the electric field is measured below $5\,\mathrm{MHz}$ ($\lambda > 60\,\mathrm{m}$). Therefore, if the shower core lies at a few hundreds of meters away from the antenna, the far-field approximation no longer applies and one has to perform an exact calculation.

In the present work, we discuss a formula for the electric field of a particle track in two semi-infinite media. This formula is valid at all frequencies. We will show that this formula reduces to the far-field (or geometrical optics) solution when the observer or the emitter are far away from the surface with respect to the observation wavelength. We will check that for most in-ice experiments with antennas near the surface that measure above $100\,\mathrm{MHz}$, the far-field approximation is satisfactory and there is no need for a near-field description. To end with, we show some results for a shower toy model and discuss the surface wave created when the shower stops abruptly upon arrival at the ground (sudden death pulse).

2. General field from a particle track in two semi-infinite media

Let us assume a three-dimensional space divided by a planar boundary at $z = 0$. Medium 1 corresponds to $z > 0$ and medium 2 to $z < 0$. Each medium has a complex relative permittivity $(\varepsilon_{1r}, \varepsilon_{2r})$, where the imaginary part indicates absorption. Both media can have a conductivity $\sigma_{1,2}$.

PoS(ICRC2019)268

Let us now consider a charge q at rest at the point $\mathbf{x} = \mathbf{x}_1$ that is instantaneously accelerated at a time $t = t_1$ to a velocity $\mathbf{v}$. After travelling in a straight line at constant speed, the particle is suddenly stopped at a time t_2 at the point $\mathbf{x}_2$. We call this trajectory a particle track, and it constitutes the basis of many radio emission Monte Carlo codes. Its current density can be written as

$$\mathbf{J}_{\text{track}}(\mathbf{x},t) = q\mathbf{v}\delta^3(\mathbf{x}' - \mathbf{x}_1 - \mathbf{v}(t'-t_1))[\Theta(t'-t_1) - \Theta(t'-t_2)], \tag{2.1}$$

where Θ is the Heaviside step function. Equivalently, in the frequency domain,

$$\mathbf{J}_{\text{track}}(\mathbf{x},\omega) = q\mathbf{v}\int_{t_1}^{t_2} \mathrm{d}t'\, e^{i\omega t'}\delta^3(\mathbf{x} - \mathbf{x}_1 - \mathbf{v}(t'-t_1)). \tag{2.2}$$

Eq. (2.2) can be regarded as an integral of successive point unit dipoles, each one with a current given by

$$\mathbf{J}_{\text{dipole}}(\mathbf{x},\omega) = \hat{z}\delta(x)\delta(y)\delta(z-z')\delta(\omega), \tag{2.3}$$

which suggests that the field for a particle track can be written as a superposition of solutions for the dipole case. The solution for the field of a dipole in two semi-infinite media can be found in [13, 14]. We assume that the velocity of the particle is, without loss of generality,

$$\mathbf{v} = v_x\hat{x} + v_z\hat{z} \equiv v(\cos\theta\hat{x} + \sin\theta\hat{z}), \tag{2.4}$$

which means that the field can be written as a composition of vertical ($\hat{z}$) and horizontal ($\hat{x}$) dipoles. Let $\mathbf{E}_{v(h)}(\mathbf{x},\mathbf{x}',\omega)$ be the field created by a vertical (horizontal) unit dipole at $\mathbf{x}' = (x',0,z')$. The adapted formulas can be found in [14], and we will not rewrite them here due to their length. The field for a particle track can be written using the dipole fields:

$$\mathbf{E}_{\text{track}}(\mathbf{x},\omega) = \frac{qv}{1\ \mathrm{A}\cdot\mathrm{m}}\int_{t_1}^{t_2} \mathrm{d}t'\, e^{i\omega t'}\left[\cos\theta\mathbf{E}_h(\mathbf{x},\mathbf{x}'(t'),\omega) + \sin\theta\mathbf{E}_v(\mathbf{x},\mathbf{x}'(t'),\omega)\right], \tag{2.5}$$

with $\mathbf{x}'(\mathbf{t})$ the trajectory of the particle. The factor of $1\,\mathrm{A\,m}$ has been included to account for the dimensions of the unit dipole field.

If both the track and the observer are in medium 1, the field can be written as a superposition of the direct field (as if there were no boundary), the field from a perfect image and a field expressed as a Bessel integral that codifies part of the field created by the boundary:

$$\mathbf{E}_{\text{track}}(\mathbf{x},\omega) = \frac{qv}{1\ \mathrm{A}\cdot\mathrm{m}}\int_{t_1}^{t_2} \mathrm{d}t'\, e^{i\omega t'}\left[\mathbf{E}_1^d + \mathbf{E}_1^{im} + \mathbf{E}_1^{int}\right] \equiv \mathbf{E}_{\text{track}}^d + \mathbf{E}_{\text{track}}^{im} + \mathbf{E}_{\text{track}}^{int}, \tag{2.6}$$

having defined the fields as a combination of the vertical and horizontal unit dipole fields,

$$\mathbf{E}_1^{d,im,int} \equiv \cos\theta\mathbf{E}_{h,1}^{d,im,int} + \sin\theta\mathbf{E}_{v,1}^{d,im,int}. \tag{2.7}$$

The direct and image unit dipole fields in the integrand are expressable in a closed form, while the integral dipole field is a Bessel integral that is quite time-consuming and must be evaluated using special techniques (as the partition extrapolation technique, see [15]), due to the oscillatory nature of the Bessel functions. As an example, we can show that the radial component for the vertical dipole is:

PoS(ICRC2019)268

$$E_{1\rho}^{int} = \frac{i\omega\mu_0 k_2^2}{2\pi k_1^2}\int_0^\infty \frac{\gamma_1 e^{i\gamma_1(z+z')}}{N} J_1(k_\rho\rho)k_\rho^2\,\mathrm{d}k_\rho \tag{2.8}$$

Once the direct, image, and integral fields have been calculated, one must integrate Eq. (2.6) using numerical methods, in general.

If the particle is in medium 2 and the observer in medium 1, the decomposition into direct, reflected and image fields is not easily obtainable, in general. The dipole field is more easily expressed as a Bessel integral. The vertical component of the vertical dipole, for instance, is

$$E_{2\to1,z} = \frac{\omega\mu_0}{2\pi}\int_0^\infty \frac{e^{-i\gamma_2 z'}e^{i\gamma_1 z}}{N} J_0(k_\rho\rho)k_\rho^3\,\mathrm{d}k_\rho, \tag{2.9}$$

which allows to write the field for a particle track in medium 2 as

$$\mathbf{E}_{\mathrm{track},2\to1}(\mathbf{x},\omega) = \frac{qv}{1\ \mathrm{A}\cdot\mathrm{m}}\int_{t_1}^{t_2}\mathrm{d}t'\ e^{i\omega t'}\left[\cos\theta\mathbf{E}_{h,2\to1} + \sin\theta\mathbf{E}_{v,2\to1}\right]. \tag{2.10}$$

3. Direct, boundary, and total fields

It is also physically intuitive to rewrite Eq. (2.6) as a sum of direct field (without boundary) and the field created by the boundary, which is mathematically the sum of the image field and the integral field. Symbolically,

$$\mathbf{E}_{\mathrm{track}}(\mathbf{x},\omega) = \mathbf{E}_{\mathrm{track}}^{d} + \mathbf{E}_{\mathrm{track}}^{im} + \mathbf{E}_{\mathrm{track}}^{int} \equiv \mathbf{E}_{\mathrm{track}}^{d} + \mathbf{E}_{\mathrm{track}}^{\mathrm{bound}}, \tag{3.1}$$

with $\mathbf{E}_{\mathrm{track}}^{\mathrm{bound}}$ being the field created by the boundary due to the excitation from the direct field. Let us calculate the different contributions to the field from a 1.2 m long down-going electron track that stops at the boundary. Medium 1 is air ($\varepsilon_{1r} = 1.0001^2$) and medium 2 is an average soil ($\varepsilon_{2r} = 13$, $\sigma = 5\,\mathrm{mS\,m^{-1}}$). The observer is located at a radial distance of 50 m and 2 m away from the boundary, in air. We show in Fig. 1, left, the radial (x, solid lines) and vertical (z, dashed lines) components of the field from the vertical track. The field is decomposed into direct and boundary fields, and they combine to yield a non-null total field. We see that the vertical field is in fact boosted at low frequencies.

We can find in Fig. 1 right the field for the same track, but as a function of the observer radial distance and for three different frequencies.

4. Field from an underground track

We can check explicitly that the field coming from underground tracks is negligible with respect to the field from tracks in the atmosphere. This is relevant, for instance, for experiments located at a high altitude, where the air showers still contain a large number of particle when they traverse the ground. Let us place an electron track that travels 1.2 m in air with an an angle of $\pi/4$ with respect to the normal of the boundary, and traverses the ground for 0.12 m, which is a reasonable depth range for underground shower particles. The observers are at $z = 2$ m and three different radial distances. The results are found in Fig. 2, left. The field coming from the ground is orders of magnitude below the field emitted in the atmosphere. This suggests that we can safely ignore the field from underground tracks when measuring the field from air showers.

PoS(ICRC2019)268

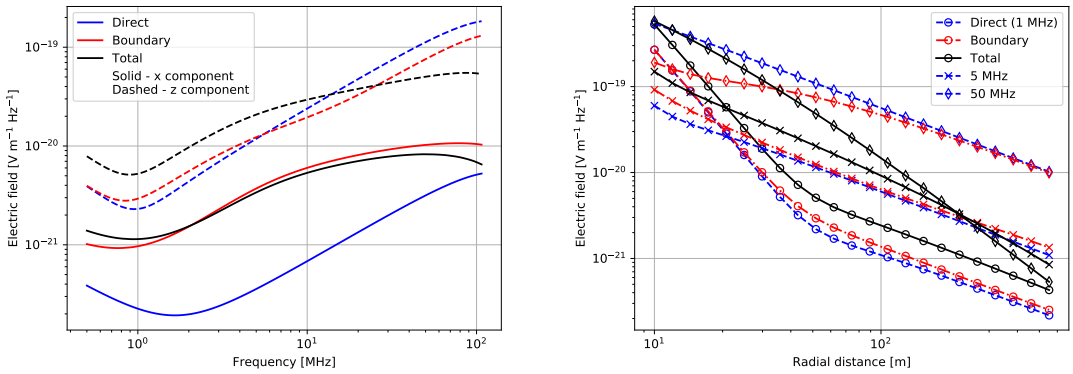

Figure 1: Left: Components of the electric field of a 1.2 m long electron track travelling at $v \sim c$. Right: same, as a function of the observer radial distance. See text for details.

5. Far field. Direct, reflected and transmitted components

When the emitting track or the observer are far away from the boundary with respect to the observation wavelength, we expect the field to be well approximated as a sum of direct and reflected components if both track and observer are in medium 1. Using the direct and image fields, this can be written as

$$\mathbf{E}^{\text{far}}_{\text{track}} = \mathbf{E}^{\text{d}}_{\text{track}} + r_{\parallel}\mathbf{E}^{\text{im}}_{\text{track},\parallel} + r_{\perp}\mathbf{E}^{\text{im}}_{\text{track},\perp}, \tag{5.1}$$

where we have introduced the Fresnel parallel ($r_{\parallel}$) and perpendicular ($r_{\perp}$) reflection coefficients.

We can check numerically whether this is the case for an antenna in ice ($\varepsilon_{1r} = 1.78^2$, we ignore absorption). We identify medium 1 as ice and medium 2 as air, and place an antenna at a distance of 2 m from the boundary, similar to an ARIANNA station, and a radial distance of 50 m. We choose several emitting down-going tracks, at heights of 10, 100 and 1000 m.

We show in Fig. 2 right the comparison between the exact field (Eq. (2.6), points) and the direct+reflected contributions (Eq. (5.1), solid lines). We have also included the ZHS-TR formalism from [16] (dashed lines). The three approaches agree in the far field. For low enough frequencies, the Fresnel approximation and the ZHS-TR method break down. However, for an experiment such as ARIANNA (observer antennas 2 m away from the boundary), whose lowest frequency is 100 MHz, we obtain that the error is $< 10\%$ for tracks in ice at a distance > 10 m, which implies that surface or near-field effects are not relevant for most in-ice showers induced by neutrinos and the far-field description is enough. However, we must remember that the present analysis is valid for homogeneous media only, and in reality ice presents a depth-dependent index of refraction. We still expect the far-field description to be valid when coupled to ray-tracing techniques, although a rigorous justification should come from FDTD techniques or advanced analytic calculations.

Analogously, if the observer lies in medium 1 and the track lies in medium 2, Eq. (2.10) can be reduced to a transmitted component in the far field. See [14] for a complete description.

6. Shower toy model and sudden death pulse (SDP

It would be useful to implement this formulas in a Monte Carlo code to get predictions on

PoS(ICRC2019)268

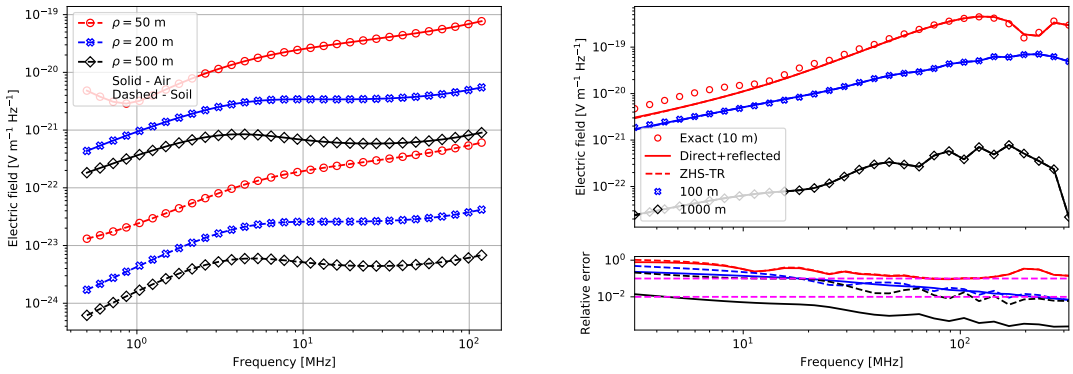

Figure 2: Left: Module of the electric field as a function of frequency for an electron track traversing the air-soil boundary and several observing radial distances. The contributions in air (solid) and soil (dashed) have been separated. Right, top: Electric field as a function of frequency created by a track in ice (several heights) with the observer also in ice at a radial distance of 100 m and a height of 2 m. Several calculations are compared. See text for details. Right, bottom: relative errors for the Fresnel and ZHS-TR approaches.

the fields induced by the boundary within a realistic EAS simulation. However, the numerical evaluation of the Bessel integrals requires a prohibitive CPU time.

Instead, we can think of a simple shower toy model to check whether there is a noticeable electric field created when a particle shower is suddenly decelerated at ground level. We model the shower as a collection of straight lines streching from an altitude of 10 km to ground level. We set these lines at several distances from the shower core: 10, 30, 50, 70, and 90 m. We expect to contain most of the particles of a vertical shower, since the Molière radius is ~ 80 m near sea level. For each radial distance, a vertical line is placed at each azimuth angle $0, \pi/4, \pi, \ldots, 7\pi/4$. There are 40 long lines in total. These lines are divided into 3 m long tracks with a charge that depends on their height:

$$q_i = -0.2 N(z_i) f(\rho_i) A_i, \tag{6.1}$$

where $N(z_i)$ is a Gaisser-Hillas profile for a 1 EeV shower, the factor -0.2 accounts for the negative excess charge, $f(\rho_i)$ is the lateral Nishimura-Kamata-Greisen distribution and A_i is a geometrical factor that depends on the area of the shower portion approximated by the line i.

This simple model calculates only the excess charge emission and not the geomagnetic component, but this is fine for the study of the SDP since it is created by the charge excess. After calculating the field in frequency domain, we filter using an eight-order low-pass Butterworth with critical frequency equal to 10 MHz and we transform it to time domain with an inverse FFT. The result is in Fig. 3. The ground altitude is 0 m, and the antennas are placed at 9 m of height, as in the EXTASIS experiment. Medium 1 is air and medium 2 is average soil. We show the direct, direct+reflected (Fresnel) and exact calculations. The first bipolar pulse is due to the shower maximum emission, for which the Fresnel calculation is close to the exact calculation. As the shower develops, the particles get closer to the boundary and the Fresnel approximation breaks down. When the particles stop at ground level, their deceleration creates the second pulse, which is the SDP discussed in [17, 18].

PoS(ICRC2019)268

It can be shown that the SDP presents two important properties: the delay between the principal pulse and the SDP is directly proportional to the distance from shower core to observer, and the amplitude of the SDP falls with the inverse of the distance to the shower core. If a SDP is measured, the core position could be reconstructed using these two properties.

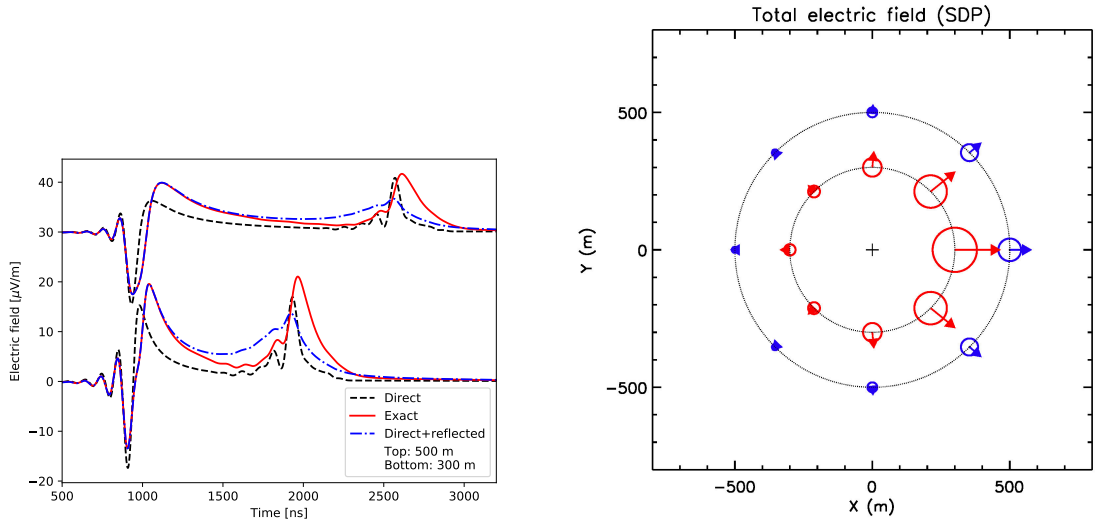

Figure 3: Left: Eelctric field in time domain created by our model shower for two different observers. The upper curve has been offset for readability. Right: Polarisation map of the SDP emitted by a 30° shower for two rings of antennas situated at 300 m and 300 m from the shower core. Arrows correspond to the horizontal polarisation, and the radius of the circles indicate the amplitude of the vertical compotent. Ground is at 1400 m of altitude.

If the shower is vertical, the SDP polarisation is vertical as well. We have also simulated a 30° shower and studied the polarisation of the SDP for this inclination. The result can be found in Fig. 3 right, from where it can be seen that the vertical polarisation is predominant.

We should clarify that the SDP seems hard to measure near sea level [12] and that its possible detection is favoured at higher altitudes such as the South Pole or the Pierre Auger Observatory site in La Pampa.

7. Summary and conclusions

We have discussed an exact solution to the electric field created by a particle track in two semi-infinite media that takes into account the effect of the boundary at all frequencies. This field is constructed using the solution for a dipole found in [13]. This field can be divided into direct emission and surface-induced emission (image field and integral field).

This solution predicts that at low frequencies, the vertical field from a particle track near ground level is enhanced and not cancelled, as one could assume calculating the direct and reflected components.

We have shown that this solution implies that the field emitted by underground tracks from an EAS is negligible compared to the emission in air.

PoS(ICRC2019)268

In the far-field, when either the track or the observer are far away from the boundary with respect to the observation wavelength, the field is well described by a superposition of direct and reflected radiation fields if track and observer lie in the same medium. This is also equivalent to the ZHS-TR formalism [16].

We have also discussed a simple toy model for air shower that supports the existence of a signal at low frequencies created when the shower abruptly stops at ground level, called sudden death pulse (SDP).

To end with, we should point out that the formulas in this work provide a way to compute the electric field of a track when a planar boundary is present, but we have not discussed the antenna response. When the field is not a pure radiation field (that is, when the antenna is in the near field), the reception patterns become more complicated and one cannot use the far-field response, in general.

Acknowledgments

We thank the Région Pays de la Loire for its financial support of the Groupe Astro of Subatech and in particular for its contribution to the EXTASIS experiment.

References

[1] F.G. Schröder, Prog. Part. Nucl. Phys. 93, 1 (2017)

[2] S. Buitink *et al.*, Nature (London) 531, 70 (2016)

[3] F. Gaté *et al.*, Astropart. Phys. 98, 38 (2018)

[4] CODALEMA collaboration, arXiv:1710.02487v1

[5] P. Schellart *et al.*, Astron. Astrophys. 560, A98 (2013)

[6] The Pierre Auger Collaboration, Phys. Rev. D 93, 122005 (2016)

[7] W. D. Apel *et al.*, Phys Lett. B 763, 179 (2016)

[8] The ARIANNA collaboration, IEEE Trans. Nucl. Sci. 62 (2015) 2202

[9] The ARA collaboration, Phys. Rev. D 83 (2016) 083003

[10] H. Schoorlemmer *et al.*, *Astropart. Phys.* 77 (2016) 32

[11] See proceedings for this conference

[12] D. Charrier *et al.*, Astropart. Phys. 113, 6 (2019)

[13] R. King, M. Owens, T. Wu, Lateral Electromagnetic Waves (Springer-Verlag, New York, 1992)

[14] D. García-Fernández *et al.*, Phys. Rev. D 99 063009 (2019)

[15] K. A. Michalski, IEEE Trans. Antennas Propag. 46, 1405 (1998)

[16] P. Motloch *et al.*, Phys. Rev. D 93, 043010 (2016)

[17] B. Revenu *et al.* in Proceedings 33th ICRC (Rio de Janeiro, Brazil, 2013)

[18] D. García-Fernández *et al.*, Phys. Rev. D 97, 103010 (2018)

PoS(ICRC2019)268